AGU PUBLICATIONS

Geophysical Research Letters

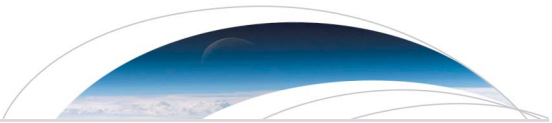

RESEARCH LETTER

10.1002/2014GL062386

Key Points:
- Spatial variability in ice sheet motion is compared with subglacial hydrology
- The proportion of annual motion that occurs in summer is spatially homogeneous
- Representation of complex hydrology in ice sheet models may be simplified

Supporting Information:
- Readme
- Table S1

Correspondence to:
A. J. Tedstone,
a.j.tedstone@ed.ac.uk

Citation:
Tedstone, A. J., P. W. Nienow, N. Gourmelen, and A. J. Sole (2014), Greenland ice sheet annual motion insensitive to spatial variations in subglacial hydraulic structure, *Geophys. Res. Lett.*, *41*, 8910–8917, doi:10.1002/2014GL062386.

Received 31 OCT 2014
Accepted 7 DEC 2014
Accepted article online 11 DEC 2014
Published online 23 DEC 2014

Greenland ice sheet annual motion insensitive to spatial variations in subglacial hydraulic structure

A. J. Tedstone[1], P. W. Nienow[1], N. Gourmelen[1], and A. J. Sole[2]

[1]School of Geosciences, University of Edinburgh, Edinburgh, UK, [2]Department of Geography, University of Sheffield, Sheffield, UK

Abstract We present ice velocities observed with global positioning systems and TerraSAR-X/TanDEM-X in a land-terminating region of the southwest Greenland ice sheet (GrIS) during the melt year 2012–2013, to examine the spatial pattern of seasonal and annual ice motion. We find that while spatial variability in the configuration of the subglacial drainage system controls ice motion at short timescales, this configuration has negligible impact on the spatial pattern of the proportion of annual motion which occurs during summer. While absolute annual velocities vary substantially, the proportional contribution of summer motion to annual motion does not. These observations suggest that in land-terminating margins of the GrIS, subglacial hydrology does not significantly influence spatial variations in net summer speedup. Furthermore, our findings imply that not every feature of the subglacial drainage system needs to be resolved in ice sheet models.

1. Introduction

One potential dynamic thinning mechanism of the Greenland ice sheet (GrIS) is surface melt-induced acceleration of ice motion [*Zwally et al.*, 2002; *Parizek and Alley*, 2004; *Andersen et al.*, 2010]. During summer, rapid increases in meltwater input from the ice sheet surface result in periods when the subglacial drainage system is more highly pressurized, leading to transient increases in basal sliding [*Bartholomew et al.*, 2011a; *Sole et al.*, 2011]. However, drainage system capacity changes in response [*Röthlisberger*, 1972; *Schoof*, 2010; *Hoffman and Price*, 2014], introducing a negative feedback which acts to lower the water pressure of the drainage system and reduce basal sliding, such that subsequent increases in basal sliding require either (a) larger meltwater pulses or (b) reductions in drainage system capacity, decreasing the quantity of meltwater required to overpressurize the system [*Cowton et al.*, 2013].

Remotely sensed observations of ice motion of a land-terminating portion of the southwest GrIS made on a single day in late summer have revealed spatially distinct flow enhancements of up to 300% relative to winter [*Palmer et al.*, 2011]. The spatial coincidence of faster flowing areas with surface drainage routing suggests that localized meltwater input to the ice bed, and the associated changes in subglacial water pressure, is the likely cause of the flow enhancement. However, point-based observations from the same region have shown that net annual ice motion is insensitive to these short-term variations in ice flow [*van de Wal et al.*, 2008; *Sole et al.*, 2013; *Tedstone et al.*, 2013], except possibly at high elevations well above the equilibrium line altitude [*Doyle et al.*, 2014]. Similarly, spatially extensive satellite observations at lower elevations have identified slower late summer flow in warmer summers but were not able to capture ice motion over a full melt year [*Sundal et al.*, 2011; *Fitzpatrick et al.*, 2013]. No study to date has therefore combined the required spatial and temporal coverage and resolution to investigate whether the insensitivity of net annual ice motion to short-term variations in ice flow holds across broader spatial scales, so the impact of spatially variable subglacial drainage and potential related flow enhancement on net annual regional ice motion remains unquantified.

Two specific aspects of surface melt-induced ice acceleration of the GrIS remain unexplored. First, while recent observations in southwest Greenland suggest that the subglacial drainage system is channelized to at least 40 km inland during summer [*Chandler et al.*, 2013], the spatial extent of surface melt-induced velocity perturbations forced by water pressure variability in these subglacial channels [e.g., *Nienow et al.*, 2005] is unknown. Second, over annual timescales it is unclear whether areas of ice close to surface meltwater input points and/or underlain by a channelized subglacial drainage system flow at a disproportionately faster rate than less hydrologically active areas. It is essential to identify whether surface

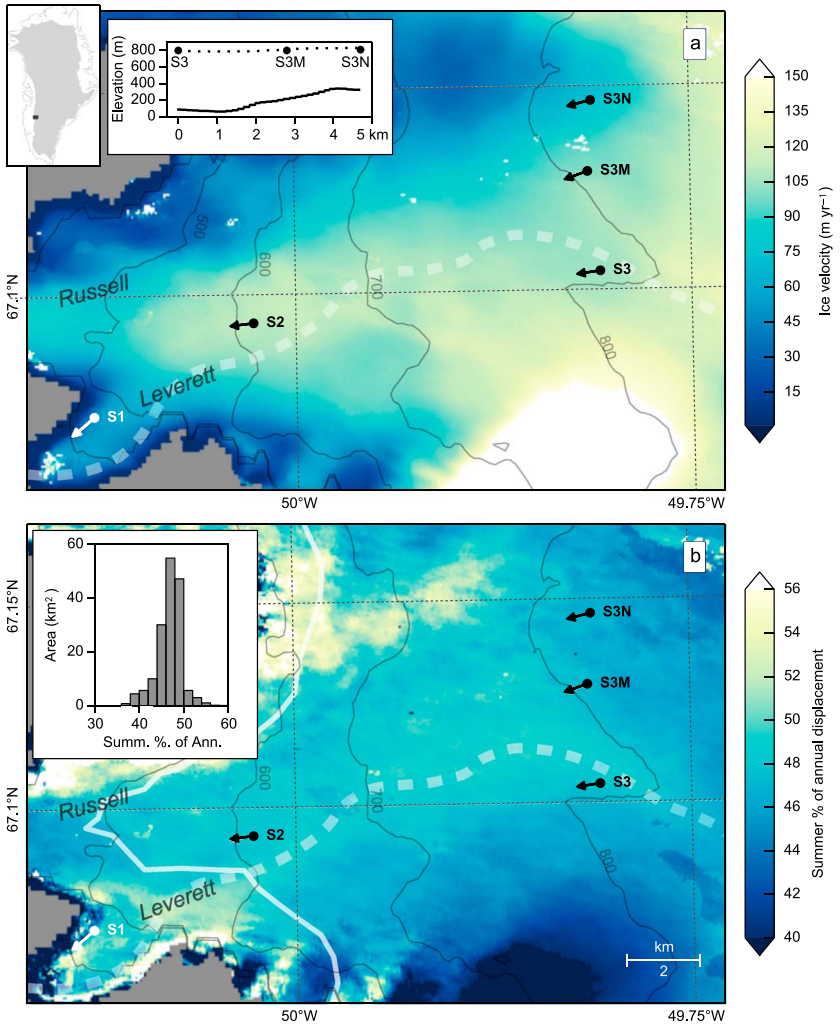

Figure 1. (a) Ice velocity (m yr^{-1}) measured by TSX/TDX during 1 May 2012 to 30 April 2013; inset: ice surface (dotted) and bed (solid) profiles through the GPS transect; outset: location of study area. (b) Summer (1 May 2012 to 31 August 2012) proportion of annual (1 May 2012 to 30 April 2013) displacement, with white line marking 2 km from the ice margin; inset: all observations further than 2 km from the ice margin as a histogram. GPS sites denoted by circles, with arrows indicating along-track flow direction; contours (in meters) from a digital elevation model derived from Operation IceBridge altimetry data [*Morlighem et al.*, 2013]; thick dashed line indicates approximate location of main subglacial channel from hydraulic potential analysis (Figure 2).

melt-induced ice acceleration has an impact on annual regional ice motion because surface melting of the ice sheet is projected to increase during the next century [*Stocker et al.*, 2013].

Here we present measurements of ice motion made during 2012–2013 at Leverett Glacier, a land-terminating glacier in the southwest of the GrIS at ~67°N (Figure 1). We measured ice motion continuously by global positioning systems (GPS) at five survey sites to examine spatial variability in the hydrological forcing of ice motion and by the TerraSAR-X/TanDEM-X (TSX/TDX) satellites over a ~20 by ~15 km area of the ice sheet margin to examine the spatial structure of seasonal and annual ice motion.

2. Data and Methods

2.1. Field Measurements

We used GPS records to observe ice motion during 2012 at three sites along a longitudinal transect (S1, S2, and S3) and at two locations transverse to the longitudinal transect ~18 km from the ice sheet margin, at ~800 m above sea level: S3M, 2.8 km and S3N, 4.7 km north of S3, respectively (Figure 1). Details of the GPS processing undertaken and longitudinal transect observations during 2012 have been described

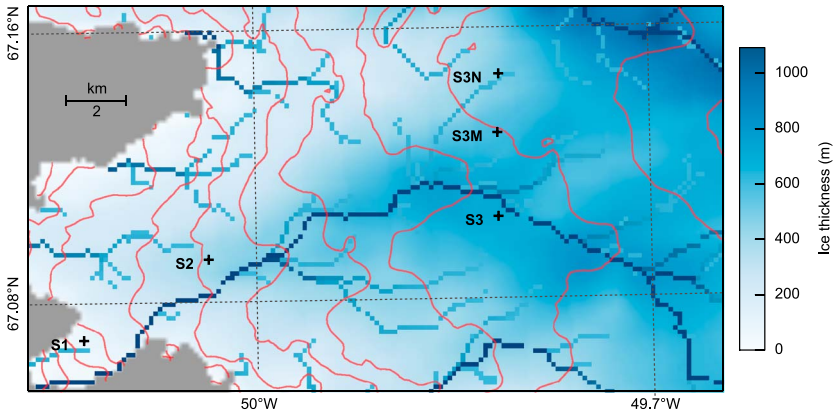

Figure 2. Ice thickness from Operation IceBridge [*Morlighem et al.*, 2013]. Subglacial hydraulic potential contours (red every 500 kPA) and major drainage pathways predicted by subglacial hydraulic potential analysis where water pressure equals ice overburden. Channel shading defined by the quantity of Upstream Contributing Cells (UCC) (values >50 UCC shown, with >1000 UCC in dark blue). Crosses denote GPS sites.

previously [*Tedstone et al.*, 2013]. GPS receiver malfunction at S3N resulted in noisy pseudo-range data, preventing accurate determination of subweekly variability in ice motion, but seasonal displacements were recorded. Additionally, power failure prevented continuous recording of ice motion at S3M between 1 July 2012 and late August 2012, restricting detailed analysis of ice motion to early summer, but absolute summer displacement was obtained. Along-track velocity uncertainties are approximately ±1 cm at each epoch and 5.2 m yr^{-1} for daily velocities [*Bartholomew et al.*, 2011a]. Seasonal trends in vertical and across-track displacement were removed by linear regression.

Air temperatures at S3 were logged every 15 min using a Campbell CR800 logger with a Campbell C107 shielded temperature probe. Discharge draining from the Leverett glacier hydrological catchment was measured using continuous water stage monitoring through a stable bedrock section and converted to discharge by calibration with repeat Rhodamine dye dilution injections, following methods described previously [*Bartholomew et al.*, 2011b].

2.2. Remote Sensing of Ice Motion

We processed synthetic aperture radar (SAR) data acquired between 26 April 2012 and 11 May 2013 by TSX/TDX into 23 ice displacement maps by applying feature tracking [*Paul et al.*, 2013] (Table S1). Our use of two tracks yields near-continuous temporal coverage but restricts spatial coverage to ~20 km inland from the ice margin. The two gaps in temporal coverage of 17 and 28 days occurred during winter (Table S1) and were filled by calculating the mean displacement of the immediately preceding and subsequent displacement maps. Steady trends in winter GPS velocities, where available [e.g., *Joughin et al.*, 2010], show that this limited averaging should not produce significant errors in ice motion estimates. Azimuth and range displacement maps were used to compute summer (1 May 2012 to 31 August 2012) and winter (1 September 2012 to 30 April 2013) displacements.

2.3. Hydraulic Potential Analysis

We used digital elevation models of the ice sheet surface and bed derived from Operation IceBridge altimetry and ice penetrating radar data [*Morlighem et al.*, 2013] to produce a theoretical reconstruction of the subglacial drainage network [*Shreve*, 1972] to complement analyses of our ice motion data. The dense radar survey in this section of the ice sheet has an average flight spacing of ~500 m and a nominal precision of 10 m for ice thickness [*Morlighem et al.*, 2013]. Calculations followed procedures outlined by *Sharp et al.* [1993]. Field observations of proglacial discharge, dye, and SF_6 tracer experiments show that most meltwater from our study area exits the ice sheet through the Leverett Glacier terminus rather than through Russell Glacier (Figure 1) [*Bartholomew et al.*, 2011a; *Chandler et al.*, 2013]. Theoretical reconstructions suggest that meltwaters from the catchment will only drain through the correct Leverett outlet when subglacial water pressure P_w is equal to ice overburden pressure (P_i) (i.e., $P_w = P_i$) (Figure 2); at lower water pressures, the meltwater exits the catchment via Russell Glacier. Despite this sensitivity, all

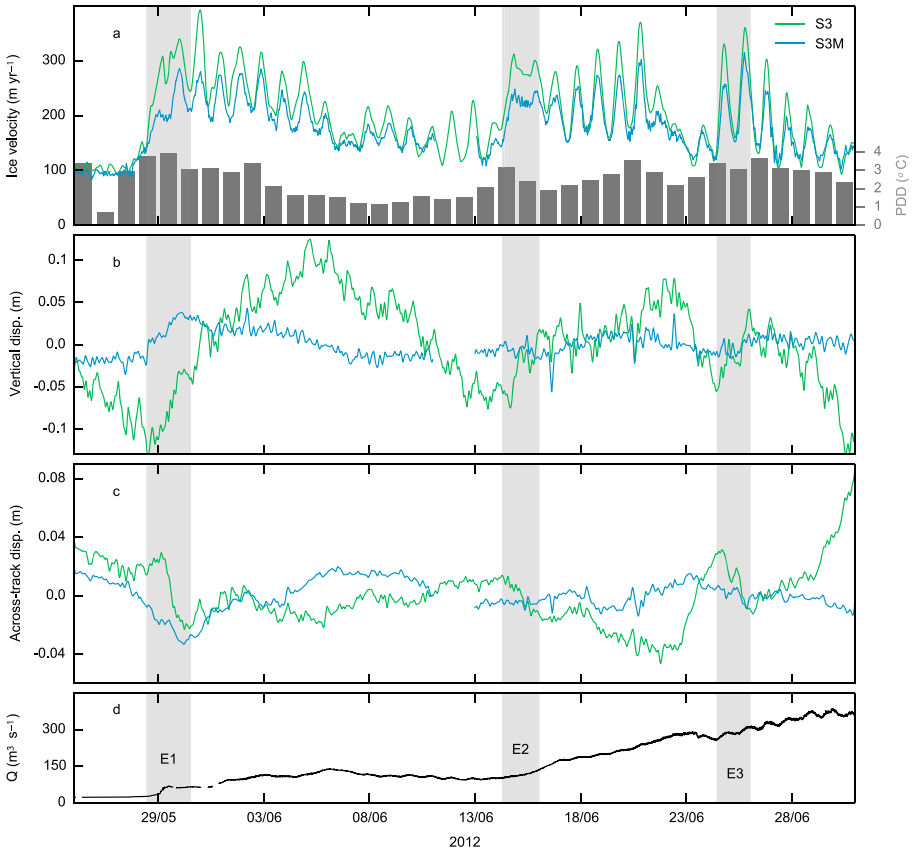

Figure 3. Time series at S3 and S3M of (a) along-track velocity and positive degree days (PDD, °C) at S3, (b) detrended vertical displacement, and (c) detrended across-track displacement. (d) Proglacial discharge hydrograph for Leverett Glacier ($m^3\ s^{-1}$).

hydraulic reconstructions predict the presence of a major drainage pathway less than 200 m north of S3, an invariance controlled primarily by the ice surface topography (Figure 1).

3. Results

3.1. Diurnal Motion at S3 and S3M

Detailed data from S3 and S3M enable us to examine the impact that spatial variability in the configuration of the subglacial drainage system has on ice motion. During the period of observation there were three clear speedup events when ice motion increased by >100% compared to the previous 2 days (Figure 3, E1–3). These pronounced speedups coincided with increasing air temperatures and rising proglacial discharge as observed in previous studies [e.g., *Iken and Bindschadler*, 1986; *Mair et al.*, 2003; *Bartholomew et al.*, 2011a].

During each event, along-track velocity at S3 increased rapidly (Figure 3a), accompanied by ice surface uplift of 5–10 cm (Figure 3b) and across-track displacement (perpendicular to the flow direction at each site shown in Figure 1) of 2–4 cm southeast (Figure 3c). While S3M's along-track velocity was 9% slower than S3 during the summer (Table 1), cross correlation of their continuous velocity records (Figure 4) shows that during each event and over the full observation period, the sites were most highly correlated at zero lag ($r > 0.8$). However, S3M only moved upward and across flow during E1, subsequently showing no resolvable signals in vertical or cross-track displacement.

After E1, S3 continued to show clear uplift and subsidence of ~2–5 cm over diurnal cycles for the remainder of the observation period but without any corresponding variability in cross-track displacement except during E2 and E3. Meanwhile, S3M did not display any systematic variability in either vertical or across-track displacement (Figures 3b and 3c).

Table 1. Ice Displacement at Observation Sites During 2012[a]

	Ice Displacement, 2012		
	Ann. (m)	Summ. (m)	Summ. %
S1	52.1	23.3	44.7
S2	110.1	50	45.4
S3	105.4	47.9	45.4
S3M	98.2	43.6	44.4
S3N	70.5	30.6	43.4

[a]Annual (Ann., meters, 1 May 2012 to 30 April 2013), Summer (Summ., meters, 1 May to 31 August), and Summer % (Summ. %, proportion of annual motion attributable to summer).

3.2. Seasonal and Annual Displacement

To identify whether spatially variable subglacial drainage during summer has an impact on ice motion over annual timescales, we examined net displacement at S3, S3M, and S3N (Table 1) during summer (1 May to 31 August 2012) and over a full year (1 May 2012 to 30 April 2013). During summer, S3 flowed fastest, with S3M and S3N flowing at 91% and 64% of motion at S3, respectively. Similarly, during the full year, S3 flowed fastest, with S3M and S3N displaced by 93% and 64% of S3, respectively. However, the *proportion* of annual displacement attributable to motion during summer varied by just 2% between the three sites. S1 and S2 (~2 km and ~8 km from the ice margin respectively) displayed equivalent behavior (Table 1) such that summer motion at all sites accounted for 43.4% to 45.4% of annual motion.

Observations of ice motion from TSX/TDX complement the GPS observations, providing much greater spatial coverage of seasonal and annual ice displacement. Over the full year, absolute ice displacement observed by TSX/TDX varied by ±2% on average of the observations recorded at each GPS site, a close agreement which validates the observations made by TSX/TDX over the rest of the study area.

The ice motion observed by TSX/TDX over the melt year (Figure 1a) reveals clear spatial variability both along and across flow, with areas of faster ice motion broadly colocated with thicker ice (Figure 2). However, there is very little variability in the proportion of annual ice displacement attributable to summer motion beyond ~2 km from the ice sheet margin (Figure 1b). There is a ~3 km wide flow zone of slightly faster (~2%) summer motion between S3 and S3M, the location of which is coincident with the subglacial drainage channel predicted by hydraulic potential analysis (Figure 2).

The homogeneous behavior of this area of the ice sheet in terms of the proportionality of summer speedup, particularly away from the thin ice margin, is clear in Figure 1b (inset). Summer displacement of 43.9–49.7% of total annual displacement, corresponding to $\bar{x} \pm 1\sigma$, accounted for 81% of variability in the study area further than 2 km from the ice margin. Areas where ice flowed proportionally faster (white in Figure 1b) or slower (dark blue in Figure 1b) during summer are restricted to marginal ice thinner than ~200 m in the former case and a steep ice fall [*Sundal et al.*, 2011] in the latter case.

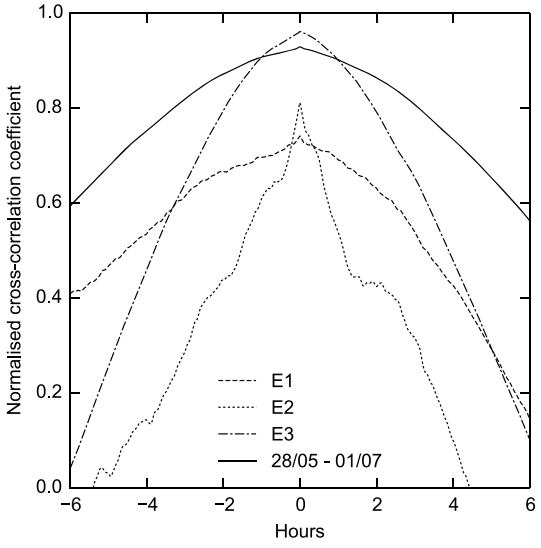

Figure 4. Cross-correlation functions between S3 and S3M during 28 May to 1 July and for events 1–3 (Figure 3), S3 as primary variable.

4. Discussion

4.1. Drivers of Diurnal Ice Motion

Observations of alpine glaciers have revealed variable pressure axes (VPAs) tens of meters wide centered on a hydraulically efficient channel, in which subglacial water pressures (P_w) vary substantially over diurnal melt cycles, in constrast to adjacent areas of the bed where P_w becomes progressively higher and less variable as the influence of the VPA declines with distance [e.g., *Hubbard et al.*, 1995; *Harbor et al.*, 1997]. At Haut Glacier d'Arolla (Swiss Alps), the highest diurnal ice surface velocities occur over the

VPA. However, the wide area over which ice velocities increase in phase with VPA P_w can only be explained by reductions in basal shear traction over a much wider (~560 m) area of the bed, requiring either an inefficient drainage system or a channelized system with many channels that hydraulically connect large areas of the bed [*Nienow et al.*, 2005].

Previous studies at Leverett Glacier have inferred the presence of an efficient, channelized subglacial drainage system to at least 40 km into the ice sheet interior during summer [*Bartholomew et al.*, 2011a; *Chandler et al.*, 2013]. The hydro-dynamical behavior observed at S3 and S3M is explicable both by the Alpine VPA framework and by hydrological modeling of the interaction between channelized and distributed subglacial drainage systems [*Werder et al.*, 2013]. S3, inferred to be in the vicinity of a major drainage pathway (Figure 2), experiences large oscillations in diurnal along-track velocity and vertical displacement, consistent with oscillatory variability in P_w. Furthermore, *Sugiyama et al.* [2010] observe that vertical ice displacement over a basal perturbation can induce a cross-track displacement at some distance away from the basal perturbation; the southeasterly displacement of S3 during the speedup periods E1–3 mimics this behavior and places S3 to the south of the VPA, in agreement with the hydraulic potential analysis.

Without additional survey sites or coupled hydro-dynamic modeling [e.g., *Hoffman and Price*, 2014], it is not possible to identify whether the fluctuations in stress regime which force synchronous along-track motion at S3 and S3M, most likely through fluctuating P_w, originate from (a) local meltwater input points or (b) fluctuations in VPA P_w forced by upglacier surface meltwater inputs. As a result, it is not possible to elucidate the relative importance of transverse stresses or the coupling lengths over which local VPA ice-bed decoupling could propagate enhanced motion away from the VPA. Nevertheless, *Werder et al.* [2013] model pressure variations up to ~ 2 km away from a subglacial channel, which would fit with our observations of a dynamic response at S3M driven by pressure variations within the inferred subglacial channel.

4.2. Seasonal and Annual Ice Motion

Our continuous observations of ice motion at S3 and S3M during 2012 confirm that, as suggested by *Palmer et al.* [2011] at the broader catchment scale, surface melt-induced ice acceleration is spatially variable over diurnal timescales. At annual timescales there is also substantial spatial variability in absolute ice motion (Figure 1a). However, it is variability in driving stress caused primarily by differing ice thickness, rather than a spatially variable drainage system, which is the cause of this variability in our study area.

Despite clear evidence for distinct subglacial channels (both from the ice motion data presented here and previous tracer studies, e.g., *Chandler et al.* [2013]) which induce complex diurnal flow patterns, the structure of the subglacial drainage system does not appear to have a significant impact on the overall extent to which summer motion contributes to annual motion. Instead, in 81% of the area further than 2 km from the ice margin, the contribution of summer motion to annual motion falls within the narrow range of ~44–50%, irrespective of proximity to underlying subglacial channels. This suggests that the surrounding regions of distributed drainage readily connect to and interact with channelized drainage features, smoothing spatial variations in velocity forced by water pressure fluctuations in the channels. Thus, the existence of channels constitutes an important control on regional subglacial water pressure, but the precise location of each channel is less important because they interact readily with the surrounding distributed drainage system rather than acting in isolation.

Our finding that an essentially spatially invariant proportion of annual motion occurs during the melt season may be explicable by both recent field observations from the GrIS and modeling. Using observations of ice velocity, moulin water levels, and borehole water pressures, *Andrews et al.* [2014] concluded that decreasing water pressures in the unchannelized (or "distributed") regions of the subglacial drainage system, not the channelized areas, were responsible for their observed late summer slowdown in ice velocities. Such hydro-dynamic coupling in unchannelized regions which underlie the majority of our study area, in contrast to narrow, discrete channelized drainage features (or VPAs), may therefore provide a plausible explanation for the spatial invariance in the proportion of annual motion which we observe during summer.

Furthermore, these observations qualitatively agree with modeling results [*Hoffman and Price*, 2014] which suggest that upon the delivery of meltwater to the ice sheet bed, ice velocity transiently increases, but a negative feedback then dominates the subsequent velocity response whereby sliding over bedrock bumps increases cavity space, lowering water pressure and in turn sliding. This negative feedback occurs even in

the absence of channelization, acting to limit the magnitude of any surface melt-driven velocity increase. Thus, the coupled hydrology dynamics of the spatially extensive unchannelized regions of the ice sheet bed may explain our observation that the summer proportion of annual ice motion is spatially invariant.

5. Conclusions

We have examined spatial variability in surface melt-induced ice motion in a land-terminating region of the southwest GrIS. We have shown that while spatial variability in the configuration of subglacial drainage controls ice motion at short timescales, these variations have negligible impact on the proportion of annual motion which occurs during summer as a result of surface meltwater inputs to the ice sheet bed. While absolute annual velocities vary substantially across the study area (due to variations in driving stress), the proportional contribution of summer motion to annual ice motion does not.

This observation is important because it implies that, for land-terminating regions of the GrIS, (1) it may not be necessary to include complex representations of subglacial hydrology in ice sheet models for simulating ice flow and (2) the placement of GPS relative to subglacial channels should only affect the detailed pattern of ice velocities over short timescales and not the relative seasonal displacement resulting from hydraulic forcing. Nevertheless, additional research needs to determine the extent to which our findings are applicable to the wider ice sheet and in particular (1) whether the invariance of ice motion to the configuration of the subglacial drainage system over annual timescales extends further inland where the extent of channelization remains equivocal [*Chandler et al.*, 2013; *Meierbachtol et al.*, 2013] and (2) the applicability of our findings to other land-terminating margins of the ice sheet and to marine-terminating margins, where hydro-dynamic coupling remains poorly understood.

Acknowledgments

We acknowledge UK Natural Environment Research Council (NERC) studentships NE/152830X/1 and NE/J500021/1 (to A.J.T.); the Carnegie Trust (P.W.N.); and from Edinburgh University, a Moss Scholarship (to A.J.T.), the Mackay Greenland Fund (A.J.T.), and the Development Trust. GPS equipment and training were provided by the NERC Geophysical Equipment Facility loan 868. Field observations are archived with the United Kingdom Polar Data Centre. The TerraSAR-X/TanDEM-X data were obtained from the German Aerospace Center (DLR) under proposal XTI_GLAC0296. M. Morlighem provided bed topography and ice thickness data. We thank the Leverett field camp members who helped with data acquisition.

The Editor thanks two anonymous reviewers for their assistance in evaluating this paper.

References

Andersen, M. L., et al. (2010), Spatial and temporal melt variability at Helheim Glacier, east Greenland, and its effect on ice dynamics, *J. Geophys. Res.*, *115*, F04041, doi:10.1029/2010JF001760.

Andrews, L. C., G. A. Catania, M. J. Hoffman, J. Gulley, M. Luthi, C. Ryser, R. L. Hawley, and T. A. Neumann (2014), Direct observations of evolving subglacial drainage beneath the Greenland ice sheet, *Nature*, *514*, 80–83, doi:10.1038/nature13796.

Bartholomew, I., P. Nienow, A. Sole, D. Mair, T. Cowton, M. King, and S. Palmer (2011a), Seasonal variations in Greenland ice sheet motion: Inland extent and behaviour at higher elevations, *Earth Planet. Sci. Lett.*, *307*, 271–278, doi:10.1016/j.epsl.2011.04.014.

Bartholomew, I., P. Nienow, A. Sole, D. Mair, T. Cowton, S. Palmer, and J. Wadham (2011b), Supraglacial forcing of subglacial drainage in the ablation zone of the Greenland ice sheet, *Geophys. Res. Lett.*, *38*, L08502, doi:10.1029/2011GL047063.

Chandler, D. M., et al. (2013), Evolution of the subglacial drainage system beneath the Greenland ice sheet revealed by tracers, *Nat. Geosci.*, *6*(3), 195–198.

Cowton, T., P. Nienow, A. Sole, J. Wadham, G. Lis, I. Bartholomew, W. F. Mair, and D. M. Chandler (2013), Evolution of drainage system morphology at a land-terminating Greenlandic outlet glacier, *J. Geophys. Res. Earth Surf.*, *118*, 29–41, doi:10.1029/2012JF002540.

Doyle, S. H., A. Hubbard, A. A. W. Fitzpatrick, D. van As, A. B. Mikkelsen, R. Pettersson, and B. Hubbard (2014), Persistent flow acceleration within the interior of the Greenland ice sheet, *Geophys. Res. Lett.*, *41*, 899–905, doi:10.1002/2013GL058933.

Fitzpatrick, A. A. W., A. Hubbard, I. Joughin, D. J. Quincey, D. Van As, A. P. Mikkelsen, S. H. Doyle, B. Hasholt, and G. A. Jones (2013), Ice flow dynamics and surface meltwater flux at a land-terminating sector of the Greenland ice sheet, *J. Glaciol.*, *59*, 687–696.

Harbor, J., M. Sharp, L. Copland, B. Hubbard, P. Nienow, and D. Mair (1997), Influence of subglacial drainage conditions on the velocity distribution within a glacier cross section, *Geology*, *25*, 739–742.

Hoffman, M., and S. Price (2014), Feedbacks between coupled subglacial hydrology and glacier dynamics, *J. Geophys. Res. Earth Surf.*, *119*, 414–436, doi:10.1002/2013JF002943.

Hubbard, B., M. Sharp, I. Willis, M. Nielsen, and C. Smart (1995), Borehole water-level variations and the structure of the subglacial hydrological system of Haut Glacier d'Arolla, Valais, Switzerland, *J. Glaciol.*, *41*(139), 572–583.

Iken, A., and R. A. Bindschadler (1986), Combined measurements of subglacial water pressure and surface velocity of Findelengletscher, Switzerland: Conclusions about drainage system and sliding mechanism, *J. Glaciol.*, *32*(110), 101–119.

Joughin, I., B. E. Smith, I. M. Howat, T. Scambos, and T. Moon (2010), Greenland flow variability from ice-sheet-wide velocity mapping, *J. Glaciol.*, *56*(197), 415–430, doi:10.3189/002214310792447734.

Mair, D., I. Willis, U. H. Fischer, B. Hubbard, P. Nienow, and A. Hubbard (2003), Hydrological controls on patterns of surface, internal and basal motion during three "spring events": Haut Glacier d'Arolla, Switzerland, *J. Glaciol.*, *49*(167), 555–567, doi:10.3189/172756503781830467.

Meierbachtol, T., J. Harper, and N. Humphrey (2013), Basal drainage system response to increasing surface melt on the Greenland ice sheet, *Science*, *341*(6147), 777–779, doi:10.1126/science.1235905.

Morlighem, M., E. Rignot, J. Mouginot, X. Wu, H. Seroussi, E. Larour, and J. Paden (2013), High-resolution bed topography mapping of Russell Glacier, Greenland, inferred from operation icebridge data, *J. Glaciol.*, *59*(218), 1015–1023, doi:10.3189/2013JoG12J235.

Nienow, P. W., A. L. Hubbard, B. P. Hubbard, D. M. Chandler, D. W. F. Mair, M. J. Sharp, and I. C. Willis (2005), Hydrological controls on diurnal ice flow variability in valley glaciers, *J. Geophys. Res.*, *110*, F04002, doi:10.1029/2003JF000112.

Palmer, S., A. Shepherd, P. Nienow, and I. Joughin (2011), Seasonal speedup of the Greenland ice sheet linked to routing of surface water, *Earth Planet. Sci. Lett.*, *302*, 423–428, doi:10.1016/j.epsl.2010.12.037.

Parizek, B. R., and R. B. Alley (2004), Implications of increased Greenland surface melt under global-warming scenarios: Ice-sheet simulations, *Quat. Sci. Rev.*, *23*(9-10), 1013–1027, doi:10.1016/j.quascirev.2003.12.024.

Paul, F., et al. (2013), The glaciers climate change initiative: Methods for creating glacier area, elevation change and velocity products, *Remote Sens. Environ.*, doi:10.1016/j.rse.2013.07.043, in press.

Röthlisberger, H. (1972), Water pressure in intra- and subglacial channels, *J. Glaciol.*, *11*(62), 177–203.
Schoof, C. (2010), Ice-sheet acceleration driven by melt supply variability, *Nature*, *468*(7325), 803–806, doi:10.1038/nature09618.
Sharp, M., K. Richards, I. Willis, N. Arnold, P. Nienow, W. Lawson, and J.-L. Tison (1993), Geometry, bed topography and drainage system structure of the Haut Glacier d'Arolla, Switzerland, *Earth Surf. Processes Landforms*, *18*(6), 557–571, doi:10.1002/esp.3290180608.
Shreve, R. (1972), Movement of water in glaciers, *J. Glaciol.*, *11*(62), 205–214.
Sole, A., P. Nienow, I. Bartholomew, D. Mair, T. Cowton, A. Tedstone, and M. King (2013), Winter motion mediates dynamic response of the Greenland ice sheet to warmer summers, *Geophys. Res. Lett.*, *40*, 3940–3944, doi:10.1002/grl.50764.
Sole, A. J., D. W. F. Mair, P. W. Nienow, I. D. Bartholomew, M. A. King, M. J. Burke, and I. Joughin (2011), Seasonal speedup of a Greenland marine-terminating outlet glacier forced by surface melt-induced changes in subglacial hydrology, *J. Geophys. Res.*, *116*, F03014, doi:10.1029/2010JF001948.
Stocker, T., et al. (2013), *Climate Change 2013: The Physical Science Basis. Contribution of Working Group I to the Fifth Assessment Report of the Intergovernmental Panel on Climate Change, Chap. Technical Summary*, Cambridge Univ. Press, Cambridge, U. K., and New York.
Sugiyama, S., A. Bauder, P. Riesen, and M. Funk (2010), Surface ice motion deviating toward the margins during speed-up events at Gornergletscher, Switzerland, *J. Geophys. Res.*, *115*, F03010, doi:10.1029/2009JF001509.
Sundal, A. V., A. Shepherd, P. Nienow, E. Hanna, S. Palmer, and P. Huybrechts (2011), Melt-induced speed-up of Greenland ice sheet offset by efficient subglacial drainage., *Nature*, *469*(7331), 521–524, doi:10.1038/nature09740.
Tedstone, A. J., P. W. Nienow, A. J. Sole, D. W. Mair, T. R. Cowton, I. D. Bartholomew, and M. A. King (2013), Greenland ice sheet motion insensitive to exceptional meltwater forcing, *Proc. Natl. Acad. Sci.*, *110*(49), 19,719–19,724.
van de Wal, R. S. W., W. Boot, M. R. van den Broeke, C. J. P. P. Smeets, C. H. Reijmer, J. J. A. Donker, and J. Oerlemans (2008), Large and rapid melt-induced velocity changes in the ablation zone of the Greenland ice sheet, *Science*, *321*(5885), 111–113, doi:10.1126/science.1158540.
Werder, M. A., I. J. Hewitt, C. G. Schoof, and G. E. Flowers (2013), Modeling channelized and distributed subglacial drainage in two dimensions, *J. Geophys. Res. Earth Surf.*, *118*, 2140–2158, doi:10.1002/jgrf.20146.
Zwally, H. J., W. Abdalati, and T. Herring (2002), Surface melt-induced acceleration of Greenland ice-sheet flow, *Science*, *297*, 218–222, doi:10.1126/science.1072708.